Development & performance enhancement of an AUV wave-charging system

Brian J. Rosenberg, Sergiy Taylakov, and Timothy R. Mundon

***Abstract*—This work presents a Wave Power Capture System (WPCS) that can be integrated into an autonomous underwater vehicle (AUV), allowing it to operate for significantly longer periods of time, potentially indefinitely. The wave-power charging capability is achieved by integrating a retractable reaction structure that can be stowed against the body of the AUV when not in use and two rotary power take-off elements housed inside the AUV. The WPCS technology is applicable to most AUV's, however this study focuses on implementation within an A-Size AUV. Of particular focus in this work is the development of different reaction plate concepts that result in enhanced wave power capture.**

***Index Terms*—AUV, reaction plate, hydrodynamics**

I. Introduction

ADOPTION of autonomous underwater vehicle (AUV) technology has recently experienced rapid growth, fueled by possibilities opened up through technology advances [1], [2]. AUVs are particularly useful as unmanned survey platforms, and typically have an array of on-board sensors to collect data for a variety of commercial and military applications. AUVs are autonomous and untethered systems and require a power source, typically batteries, to be carried onboard. An increase in available energy by even a small amount can be greatly impactful for AUV applications with benefits including longer mission durations, higher sampling rate, more sensing capability and improved communication capability. This can be accomplished through some self-recharging capability within the AUV, allowing the AUV to extract energy from its surrounding environment, and eliminating the need to recover the vehicle until the mission is complete [3].

Oscilla Power is working on developing a wave-powered recharging module that can be adapted into AUV's. This concept utilizes two rotary PTO units that are driven by two independent tendons, located axially along the body to connect the AUV to a reaction plate that is deployed autonomously when the AUV needs to be recharged. This arrangement allows both pitch and heave motion to be primary contributors to relative (power generating) motion. Additional motion in surge, sway and yaw will also result in some secondary power generation. The reaction plate will be stowed against the body of the AUV when not in use and then lowered below the AUV body to generate power.

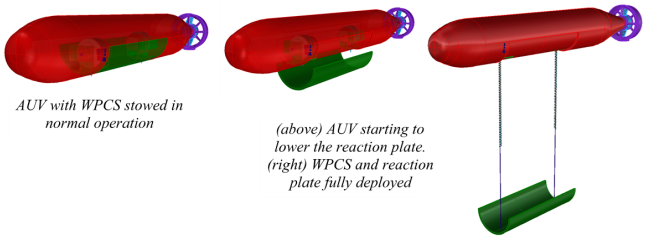

Fig. 1. A wave-powered charging concept for an AUV.

The work presented here focuses on the optimization of the hydrodynamics of the reaction plate so that power performance is maximised. Previous work has indicated that increasing the added mass of the reaction plate increases power capture [4]. The geometry of the reaction plate will be constrained so as to allow the AUV to operate normally when not deployed. This work will thus look at different modifications to the reaction plate including incorporating multiple 'nested' reaction plates that mate together when stowed, as well as adding longitudinal fins that will not impede normal streamwise flow when operating. The light weight of the reaction plate relative to its area means that there may be a tendency for the tendons to experience snap loading in cases where the reaction plate does not fall as fast as the AUV body. This work further investigates the incorporation of adaptable geometry, such as a reaction plate that folds inward on the downward travel, significantly reducing the hydrodynamic resistance.

A series of experiments will be presented in which the different reaction plates are sinusoidally forced in a quiescient basin to characterize the hydrodynamic coefficients over a range of representative frequencies and amplitudes. Finally, a time-domain model, informed by the hydrodynamic coefficients measured experimentally, will be used to calculate AUV power performance in different sea states, and will be used to evaluate the effect of the different reaction plate modifications.

II. Concept for wave-power charging system

The goals of this work are to develop a practical design for a Wave Power Capture System (WPCS) that is adaptable to fit into suitable AUV's and to identify potential methods to maximise power capture. This work focuses specifically on a module that offers a self-charging capability for the A-Class AUV in an energetic

This work was supported by the U.S. Department of Energy (Funding Agreement No DE-SC0020867)

B. J. Rosenberg is with Oscilla Power Inc. 4240 Gilman Pl W, Suite B, Seattle, WA 98103 U.S.A (e-mail: rosenberg@oscillapower.com).

T. R. Mundon is with Oscilla Power Inc. 4240 Gilman Pl W, Suite B, Seattle, WA 98103 U.S.A (e-mail: mundon@oscillapower.com).

Digital Object Identifier:
https://doi.org/10.36688/ewtec-2023-540

Fig. 2. A-size AUV.

TABLE I
PROPERTIES OF A-SIZE AUV

Quantity	Value
Baseline Length	0.91 m
Diameter	0.124 m
Mass	10 kg

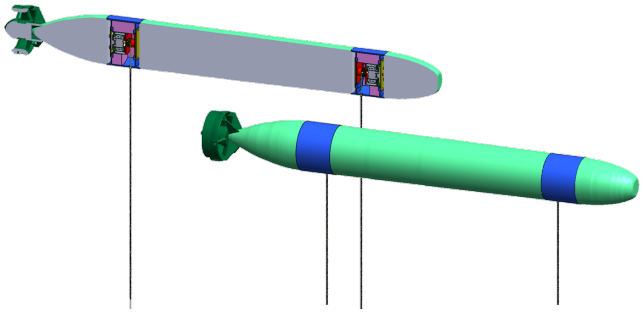

Fig. 3. Location of the WPCS modules (shown in blue) within the AUV

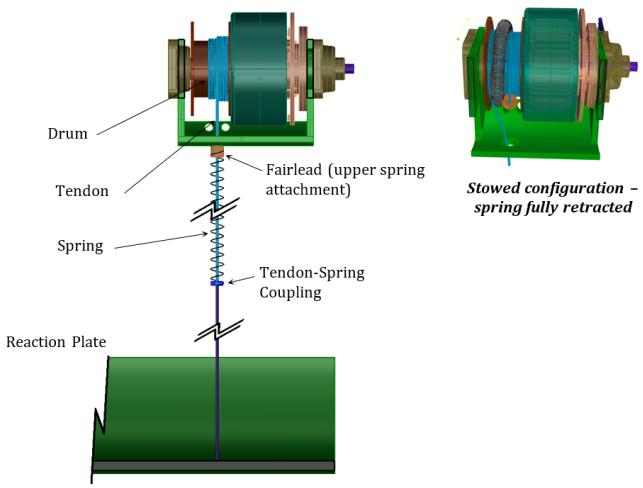

Fig. 4. Tendon configuration showing spring attachment.

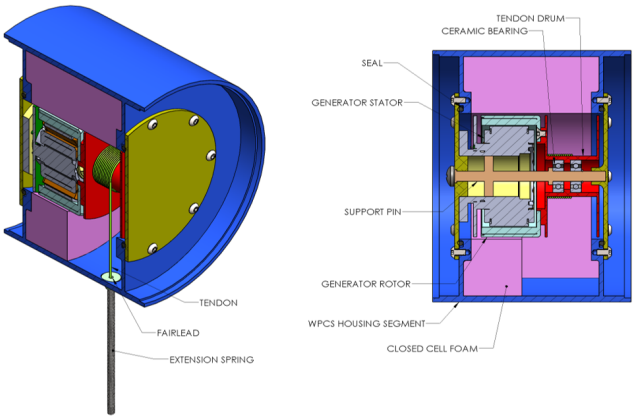

Fig. 5. Detailed model of WPCS module

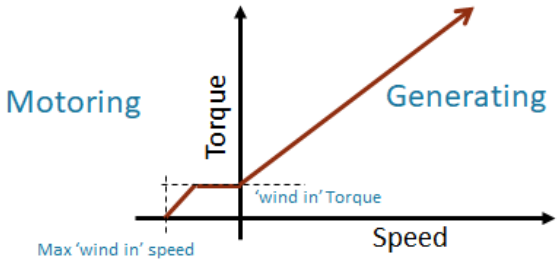

Fig. 6. Generator control profile.

ocean wave environment. The A-size form factor is summarized in Figure 2 and Table II.

The WPCS architecture is roughly based on Oscilla's multi-mode point absorber concept [4]. The system uses two tendons connecting to a reaction plate (rather than three as in the Triton architecture) as shown in Figure 1 and 3. Each tendon applies torque to a generator by winding onto a drum as shown in Figure 4 and 5. An efficient brushless DC motor/generator is used at the core of the WPCS to extract the power from the system when it is excited by waves. As the amount of space available in the AUV is likely very limited, it is assumed that the body of the AUV can be extended by the addition of the WPCS modules. Two separate WPCS modules are used, one located at the front of the AUV and the other at the rear, one per tendon. Each WPCS module contains a PTO module and required control as an isolated compartment or 'segments' that can be inserted into the body of the AUV. Importantly, any addition made to the AUV must not affect the AUV during normal (non-charging) operation. Thus the two WPCS modules and reaction structure must together be neutrally buoyant.

A two-body WEC also requires a restoring force to balance the mass of the reaction plate in equilibrium. In order to allow a significant amount of relative displacement, an external mechanical extension spring is used. However, for this also to fit within the physical envelope, it is installed concentric to the tendon allowing it to be wound on and off the drum during recovery/deployment. Figure 4 shows the stowed configuration where the fairlead and spring are wrapped around the generator drum.

Due to the tendon-spring arrangement, the generator extracts power during relative separation of the AUV and reaction structure, so the generator must also act as a motor to take in the tendon slack when the two bodies move towards each other. The amount of power required to wind in the tendon is expected to be mini-

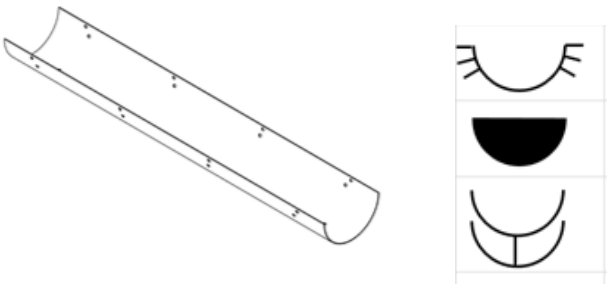

Fig. 7. (Left) Baseline reaction structure. (Right) Modifications to the baseline design that aim to increase added mass: (top) streamwise fins (middle) 'end-caps' (bottom) dual tandem structures

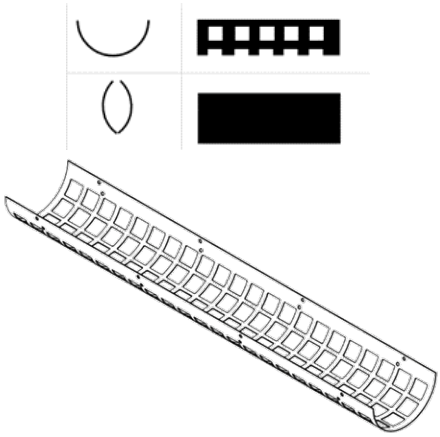

Fig. 8. Simplified representations of morphable structures (slotted and folding)

mal, however this functionality must be implemented after each generating stroke to enable power extraction on the subsequent generating stroke.

The control logic is summarized in figure 6. In power extraction (generating) mode, the controller implements a linear damping relationship between torque and speed. This allows the WEC to absorb mechanical energy efficiently from the waves. In motoring mode, the controller implements a minimal amount of motoring torque, ideally at a constant speed, to wind in the tendon and maintain a minimum tension.

III. Reaction plate geometries

A. Baseline reaction plate

The reaction plate will be stowed against the body of the AUV when not in use and then lowered below the AUV body when required to generate power. The geometry of the reaction plate will be constrained so as to allow the AUV to operate normally when not deployed. This naturally gives the plate a semicircular U-shape. The 'baseline' reaction structure shape will be considered a simple extruded U-shape as shown in Figure 7. This work will look at how different modifications to the baseline reaction plate may improve charging performance without affecting normal AUV operation when stowed.

B. Modifications to baseline reaction plate

Increasing the hydrodynamic added mass of a reaction structure can increase its reaction force, leading to improvements in power capture [4]. In addition to changing the overall geometry, the literature further indicates that mild changes to the edges of the plate can also be used as a mechanism of increasing the added mass [5]. Three modifications to the baseline reaction structure are proposed, summarized in Figure 7, that aim to increase its hydrodynamic mass:

1) Incorporating dual tandem U-shaped reaction structures that 'nest' together when stowed. Here two structures were considered, but potentially more can be incorporated depending on the allowable thickness of the stowed plate.
2) Incorporating multiple streamwise ribs, i.e. longitudinal fins along the length of the reaction structure. The intent is that that these fins will not impede normal streamwise flow when the AUV is operating, however they will enhance the reaction structure's vertical added mass when in charging mode.
3) Incorporating semi-circular 'end-caps' at the front and rear end of the reaction structure with the aim to entrain more fluid. Such end-caps would be hinged and spring-loaded so that they retract into the reaction structure when stowed.

The light weight of the reaction structure relative to its area means that there may be a tendency for the tendons to experience slack loading in cases where the reaction plate does not fall as fast as the AUV body. As a potential solution to this issue, this work investigated the incorporation of a morphable geometry, that can have asymmetric hydrodynamics depending upon the direction of travel. To explore this concept, two morphable geometries were considered:

1) A reaction structure that folds inward on the downward travel, and
2) A reaction structure that is solid or slotted depending on direction of motion by means of hinged plates over the slots. Each 'pore' in the reaction structure in practice would have a thin plastic cover with a living hinge bonded to the reaction structure.

As a simplified model, we measured the hydrodynamics of these structures 'locked' in their low-resistance state shown in Figure 8. Then, a comparison with the baseline reaction structure hydrodynamics can allow the creation of a synthetic hydrodynamic profile, whereby the structure behaves like the baseline shape while traveling up and like the low-resistance shape while travelling down. While this simplified representation does not capture all the necessary dynamics, i.e. the hydrodynamics would depend on the phasing and time constant of the hinging which would need to verified experimentally, the experiments here were designed to give an indication of the degree of asymmetry attainable.

IV. Forced oscillation experiments

Heave plate hydrodynamics can be nonlinear (amplitude dependent) and poorly resolved with some nu-

Fig. 9. Reaction plate test articles laser cut from aluminum

Fig. 10. Measurement and Optimization of Reaction Plate Hydrodynamics (MORPH) Laboratory.

merical tools [6]. To accurately characterize the reaction plate hydrodynamic forces over a range of oscillation regimes, a plunging test appartus was used, shown in Figure 10. The test facility, known as the Measurement and Optimization of Reaction Plate Hydrodynamics (MORPH) Laboratory, consists of a quiescent water basin (5000-gallon 4 m in diameter, 2 m in depth) in which a full-scale AUV reaction structure (Figure 9) is vertically oscillated using a pair of ball-screw linear actuators. The ability to test full-scale reaction structure articles enables accurate measurement of hydrodynamic properties for use in numerical models.

The actuators provide up to 100mm of travel and are each controlled by a servo motor and a feedback control system. A master displacement signal for both actuators is provided by an analog waveform generator built into the servomotor PID controller (Parker 6K-2), which was followed using encoder feedback from the motors.

The implementation of two actuators allows the exploration of multi-modal response, similar to what would be experienced in AUV charging system. Oscillating the two actuators in phase enables characterization of the translational drag and added mass (heave), while oscillating the actuators 180° out of phase enables characterization of the rotational drag and added moments of inertia. For this work, only sinusoidal heaving motions were performed, however future work will look at rotational (pitch) motions.

Cylindrical support arms are connected between each actuator and the reaction structure at the point where the tendons would connect, as shown in Figure 10. Each support arm is supported by a sleeve bearing to prevent any lateral motion, and load cells were installed between the bottom of each arm and the top of the test plate. A direct measurement of the linear displacement of each actuator, relative to the stationary gantry, was made using an analog string potentiometer. The total force required to oscillate the reaction plate in water (which includes contributions from the hydrodynamic resistance force as well as the structural inertia of the rig components beneath the load cell) is measured using an S-beam load cell on each support arm. The displacement and force analog signals were simultaneously acquired at 1 kHz using a National Instruments DAQ running Labview software.

Each test article was sinusoidally oscillated over a range of wave heights (0-100mm in increments of 10mm) and wave periods (1s, 2s, 4s). Tests were executed for 15 wave cycles and the last 10 cycles were phase averaged to calculate the hydrodynamic coefficients, added mass and drag, as described below.

V. Results - Reaction Plate Hydrodynamics

For each reaction structure tested, key hydrodynamic coefficients were obtained as functions of the two governing nondimensional parameters, Keulegan Carpenter number (KC) and Reynolds number (Re) [7]. Experiments (regular sine waves) were performed over a range of representative KC and Re, where:

$$KC = \frac{2\pi \cdot z}{D} \tag{1}$$

and

$$Re = \frac{2\pi f \cdot z \cdot D}{\nu} \tag{2}$$

In equations 1-2, z is the oscillation amplitude, f is the oscillation frequency, D is a characteristic length scale and ν is the kinematic viscosity of water. For this study, the reaction structure diameter was taken as the relevant characteristic dimension.

Characterizations of the key hydrodynamic properties (drag and added mass) are derived by fitting the experimental data to a Morison formulation [8]. The Morison formulation is a heuristic model that decomposes the net hydrodynamic force into an inertial term, which is in phase with acceleration, and a drag term that is proportional to the (square of the) velocity.

$$F = \rho C_a V \dot{u} + \frac{1}{2}\rho C_d A u\,|u| \tag{3}$$

The added mass coefficient C_a and drag coefficient C_d are then obtained through a least squares fit to equation 3 using the measured hydrodynamic force F, velocity (u) and acceleration ($\dot{u}$). The characteristic area, A, is taken to be the projected cross-sectional area in the vertical direction, and the characteristic volume V is taken to be the volume of a cylinder with length and diameter equal to the baseline reaction structure. A consistent reference area and volume were used for all reaction plate variants.

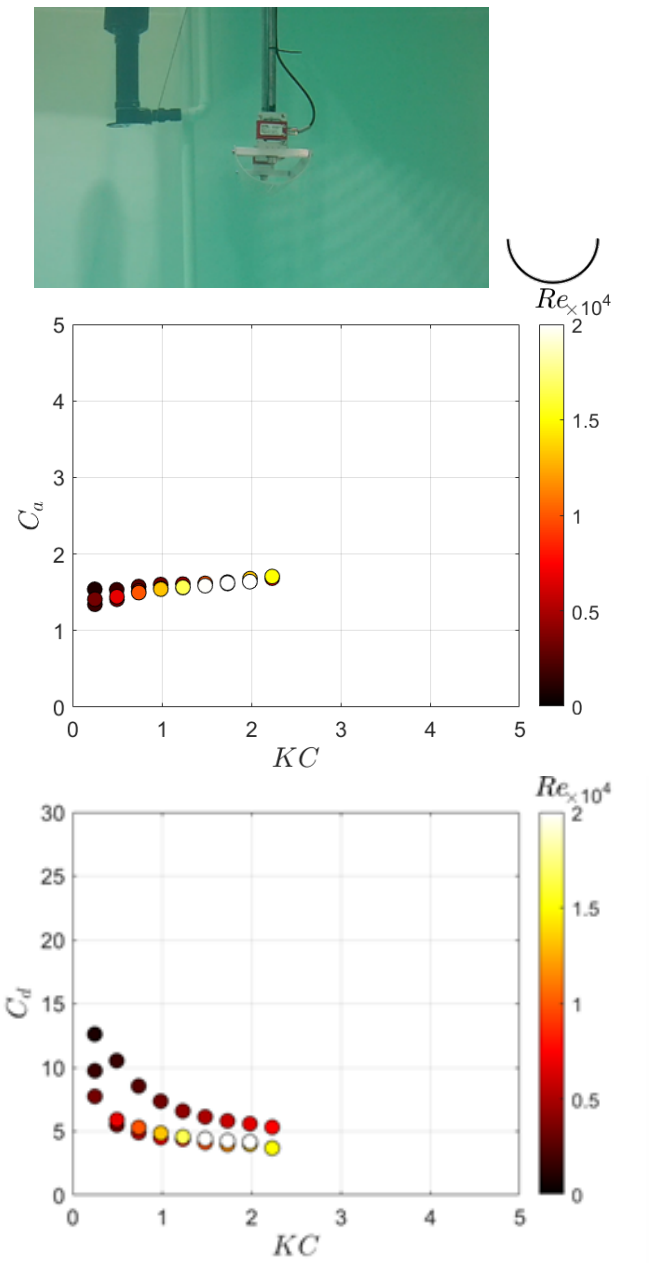

Fig. 11. Baseline-U reaction structure. In the C_d profile, the upper curve (lower Re) corresponds to the 4s period oscillations, and the lower two curves (higher Re) correspond to the 1s and 2s period oscillations.

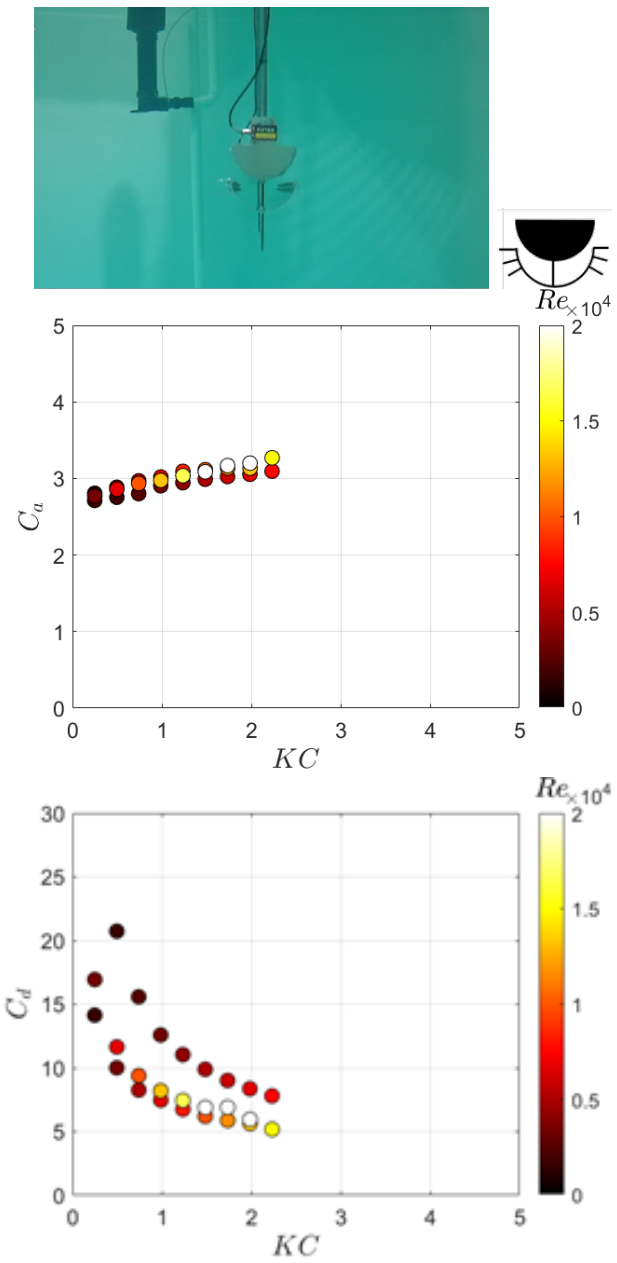

Fig. 12. Reaction structure with 2 nested-U's, endcaps, and streamwise ribs. In the C_d profile, the upper curve (lower Re) corresponds to the 4s period oscillations, and the lower two curves (higher Re) correspond to the 1s and 2s period oscillations.

Figure 11 presents the hydrodynamic coefficients for the baseline reaction structure. With regards to Reynolds number, the added mass is fairly independent. The drag coefficient, on the other hand, is higher at lower Re, for the 4s oscillation period tests, but appears to converge at higher Re, for the 2s and 1s oscillation period tests.

Both the added mass and drag coefficients display nonlinear, amplitude-dependent behavior. The C_d appears to slowly plateau at high KC, however the added mass appears to continually increase with KC. This has important implications in modeling the AUV system because typical computational tools (BEM) assume linear potential flow theory with infinitesimally small oscillation amplitudes. The result obtained here experimentally, shows that the added mass is higher for larger oscillation amplitudes.

It should be noted that, due to limitations in the actuator stroke, only a limited KC range was attainable in these laboratory measurements. In an energetic wave environment, it is expected that the reaction structure would achieve KC values 5 times larger than the values obtained here. Future work will be aimed at upgrading the actuators to longer travel and extending these curves to more realistic oscillation amplitudes.

The hydrodynamic coefficients for the best-performing (highest added mass) reaction structure shape are shown in Figure 12. Similar trends are evident, although there is a more distinct increase in C_a with KC (amplitude) which adds further import to testing at higher KC values.

Figure 13 summarizes the added mass coefficients for the baseline and proposed modified reaction struc-

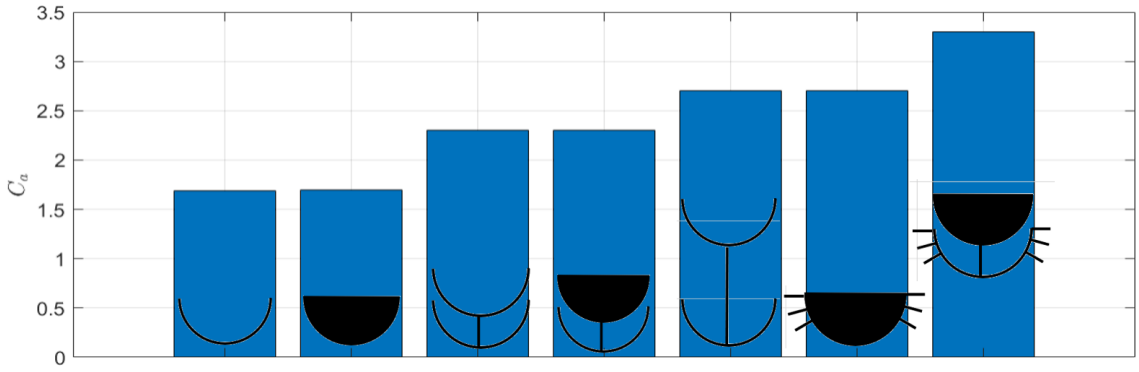

Fig. 13. Added mass comparison for various reaction structure configurations (KC =2.2). The symbols overlaid on each bar correspond to the reaction structure concepts summarized in Figure 7 and 8

TABLE II
SUMMARY OF REFERENCE LOCATIONS AND MOST PROBABLE WAVE CONDITIONS

Region	Reference Location	Flux $[kW/m]$	$T_p[s]$	$H_s[m$
West Coast	PMEC, Oregon	37.9	10.6	1.75
West Coast	WETS, Oahu	13.8	7.7	1.75
Great Lakes	Lake Michigan	2.4	4.9	0.75
Gulf of Mexico	East Gulf	6.0	4.9	0.75
East Coast	New Hampshire	9.0	4.9	1.25

tures shown in Figure 7. All data are reported for a consistent oscillation amplitude, $KC = 2.2$. An interesting conclusion from this work is that that the end-caps have minimal impact on the heave added mass. This may be due to the high aspect ratio of the reaction structure such that end-effects are small and additional fluid entrainment at the ends does not make a meaningful difference. However, results in Figure 13 clearly indicate that incorporating multiple nested U-structures as well as longitudinal fins can significantly increase the added mass. Furthermore, combining these features in different ways can further increase the added mass.

Relative to the baseline state, both morphable structures exhibit nearly an order of magnitude reduction in added mass in their morphed state (slotted or folded), as shown in Figure 14. The slotted version has a 73% reduced drag coefficient, and the folded state has a 90% reduced drag coefficient relative to the baseline state.

VI. NUMERICAL MODELING SUMMARY

For the purposes of this project, we considered deployment of the AUV/WPCS system in a wide variety of potential reference locations in the US. Typical climates were considered from the US West Coast (WETS and PMEC), Great Lakes, Gulf of Mexico, and the US East Coast (New Hampshire)

To generate a single representative design wave condition at each deployment location, the most common wave condition for each location was used. This wave condition was determined by calculating the most probable (H_s, T_p) pair from the joint probability distribution derived from at least 1 year of NDBC hindcast data at each deployment location.

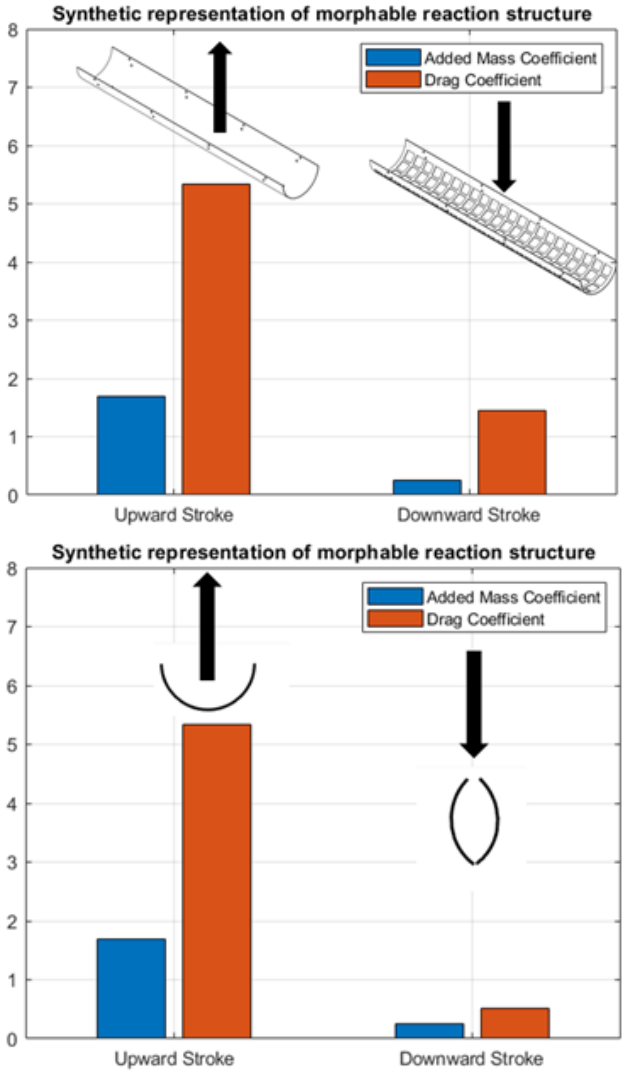

Fig. 14. Hydrodynamics of morphable structures. This simplified synthetic model is for a single amplitude (KC = 2.2) and oscillation period (T = 4s). (Top) Structure with multiple hinged flaps. (Bottom) Folding structure.

A summary of the most probable wave condition at each reference location is summarized in Table II. From this analysis, it can be seen that the design wave conditions for the Great Lakes and Gulf of Mexico are the same. The East Coast reference location (New Hampshire) displayed two peaks in the wave scatter

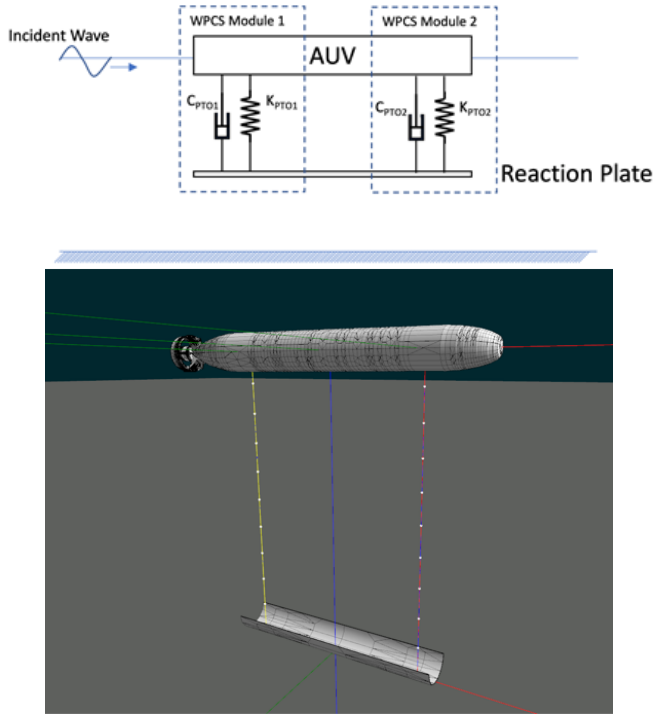

Fig. 15. (Top) WPCS free body diagram illustrating the two PTO elements. (Bottom) Time-domain hydrodynamics model developed in ProteusDS

diagram from the wind-wave and the swell-wave component. The shorter period wind-wave component was selected for this analysis as it is slightly more common.

While these reference locations encompass a wide variety in energy content (more than an order magnitude), the lower energy sites tend to have shorter period waves closer to the natural period of the WEC. Since the WEC has greater wave-to-mechanical capture efficiency in the shorter period regime, it is not necessarily the case that the best performance will be linked to the most energetic sites.

To evaluate overall performance of the system, including generation of design loads and power metrics, a full hydrodynamic numerical model of the AUV and WPCS was developed in Proteus DS and Orcaflex time domain modeling software, cross-validated against each other (Figure 15). Reaction structure hydrodynamic parameters, determined from the forced oscillation tests presented above, were used to inform the numerical model. Given that the typical operating wave height is substantially larger than either the AUV or reaction plate characteristic dimensions, non-linear effects will become important. Accordingly, non-linear buoyancy and Froude-Krylov forces on the AUV body were included in the numerical model.

The model was used to calculate the power performance using the baseline reaction structure shape and to understand how the power changes by incorporating the different modifications studied in this project.

Table III summarizes the mean mechanical power (normalised) at each of the deployment sites for the baseline reaction structure and the improved reaction structure that enhances the added mass using dual nested-U's and longitudinal fins.

TABLE III
AUV CHARGING POWER (NORMALISED) IN VARIOUS US CLIMATES USING THE BASELINE OR OPTIMISED REACTION STRUCTURE (DUAL NESTED-U'S WITH LONGITUDINAL FINS)

US Climate	Baseline	Optimized
PMEC, Oregon	0.105	0.375
WETS, Oahu	0.2325	0.825
Lake Michigan	0.22	0.5
East Gulf	0.22	0.5
New Hampshire	0.375	1.0

On average, the improved reaction structure provides a 2.9 times improvement in charging rate compared to the baseline reaction structure.

With regards to choice of climate, it can be seen that the AUV generates the most power in the short-period wind waves off the US East Coast. Interestingly, while the Oregon site has the highest wave resource, the AUV absorbs the least amount of power here since the longer period waves are further from the system natural period.

VII. CONCLUSION

This work has developed a concept that will allow a small AUV to recharge its batteries using ocean waves. Importantly, this concept is self-contained and requires no external infrastructure to operate, allowing the AUV complete freedom to operate. Further, the proposed approach is scalable and adaptable and can potentially be applied to any AUV.

Of particular interest in this work was the development of an improved reaction structure that was able to contribute significantly to the power capture. Relative to a baseline U-shaped reaction structure, it was found that adding streamwise ribs along the length of the structure as well as incorporating dual tandem U-shaped reaction structures, which nest together when stowed, can significantly enhance the hydrodynamic mass provided by the reaction structure. When both innovations are applied together, this results in increased reaction forces provided by the reaction structure leading to improvements in power capture. Importantly, these modifications do not affect performance when the AUV leaves charging mode and re-enters normal operating mode.

Dynamically morphable structures were considered at simple level, and we anticipate that future work will be able to take full advantage of these types of structures. Forced oscillation tests using a tendon will be especially useful in assessing the impact of hydrodynamic asymmetry on WEC performance.

REFERENCES

[1] N. Muchiri and S. Kimathi, "A review of applications and potential applications of uav," in *Proceedings of sustainable research and innovation conference*, 2016, pp. 280–283.

[2] J. Nicholson and A. Healey, "The present state of autonomous underwater vehicle (auv) applications and technologies," *Marine Technology Society Journal*, vol. 42, no. 1, pp. 44–51, 2008.

[3] B. P. Driscol, A. Gish, and R. G. Coe, "Wave-powered auv recharging: A feasibility study," in *ASME 2019 38th International Conference on Ocean, Offshore and Arctic Engineering*. American Society of Mechanical Engineers Digital Collection, 2019.

[4] T. R. Mundon, B. J. Rosenberg, and J. van Rij, "Reaction body hydrodynamics for a multi-dof point-absorbing WEC," in *12th European Wave and Tidal Energy Conference (EWTEC2017)*, 2017.

[5] C. J. Rusch, T. R. Mundon, B. D. Maurer, and B. L. Polagye, "Hydrodynamics of an asymmetric heave plate for a point absorber wave energy converter," *Ocean Engineering*, vol. 215, p. 107915, 2020.

[6] J. Li, S. Liu, M. Zhao, and B. Teng, "Experimental investigation of the hydrodynamic characteristics of heave plates using forced oscillation," *Ocean Engineering*, vol. 66, pp. 82–91, 2013.

[7] G. H. Keulegan and L. H. Carpenter, "Forces on cylinders and plates in an oscillating fluid," *J. Res. Nat. Bur. Stand.*, vol. 60, no. 5, May 1958.

[8] J. Morison, J. Johnson, S. Schaaf *et al.*, "The force exerted by surface waves on piles," *Journal of Petroleum Technology*, vol. 2, no. 05, pp. 149–154, 1950.